**Wuhan University Journal of Natural Sciences**

2026, Vol.31 No.2, 157-165

Article ID 1007-1202(2026)02-0157-09 DOI https://doi.org/10.1051/wujns/2026312157

Cite this article: QIAN Jing, WEI Zhen, ZHENG Wei, *et al*. Observation on the Embryonic and Larval Development of *Leiocassis longirostris* and Determination of Its Point of No Return under Starvation[J]. *Wuhan Univ J of Nat Sci*, 2026, 31(2): 157-165.

# Observation on the Embryonic and Larval Development of *Leiocassis longirostris* and Determination of Its Point of No Return under Starvation

**QIAN Jing[1], WEI Zhen[2] , ZHENG Wei[2†], XIONG Yinlin[2], JIANG Menghao[2], LI Na[1], TAO Min[1], QIN Chuanjie[1]**

1. Fishes Conservation and Utilization in the Upper Reaches of the Yangtze River Key Laboratory of Sichuan Province, College of Fisheries, Neijiang Normal University, Neijiang 641100, Sichuan, China;

2. Center for Conservation and Utilization of Rare and Endemic Fishes in Sichuan, Chengdu 611247, Sichuan, China

**Abstract:** To investigate the embryonic and larval developmental characteristics of *Leiocassis longirostris* (*L. longirostris*) and determine the Point of No Return (PNR) of starved larvae, fertilized eggs were cultured in a recirculating glass aquarium maintained at a water temperature of (24.5 ± 0.5) ℃. Respectively, the chronological characteristics of embryonic and larval development were observed under a microscope, and starvation experiments were conducted on newly hatched larvae to study their morphological development, growth traits, and feeding capacity. The results indicated that the fertilized eggs of *L. longirostris* reached a diameter of (3.46 ± 0.16) mm after water absorption and swelling, and the embryonic incubation period was 68-70 h. Embryonic development was observed to progress through eight consecutive stages: fertilized egg, cleavage, blastula, gastrula, neurula, organogenesis, pre-hatching, and hatching. Subsequently, we observed that newly hatched larvae undergo three distinct developmental phases before initial feeding: the appearance of body pigments, the formation of the intestinal tract, and the first coiling of the intestinal tube. Thereafter, results from the larval starvation experiment indicated that *L. longirostris* larvae relied on endogenous nutrition within the first 4 days post-hatching (dph). Initial feeding occurred at 5 dph, with a feeding rate of (63.33 ± 2.89)%, marking the onset of the mixed nutritional stage. By 9 dph, the yolk sac was fully absorbed, and the larvae transitioned to exclusive exogenous nutrition. Moreover, the feeding rate remained at 100% from 8 to 11 dph, followed by a decline. The PNR was identified at 16 dph. Subsequently, complete starvation-induced mortality occurred between 16 and 17 dph. Thus, the optimal initial feeding time for *L. longirostris* larvae is recommended to be 5 dph. In summary, the findings of this study provide fundamental data on the early developmental stages of *L. longirostris*, which has significant practical implications for improving larval rearing efficiency in aquaculture.

**Key words:** *Leiocassis longirostris*; embryonic development; larval development; Point of No Return (PNR)

**CLC number:** S965

**Received date:** 2025-09-15 

**Foundation item:** Supported by Sichuan Science and Technology Program (2025NZZJ0002) and the Project Entitled Investigation into the Early Developmental Growth of *Leiocassis longirostris* and the Effects of Nitrogen Pollutants on them (HXL-240033)

**Biography:** QIAN Jing, female, Ph. D., research direction: aquaculture. E-mail: jingq1992@163.com

† Corresponding author. E-mail: zhengwei1991a@163.com

# 0 Introduction

*Leiocassis longirostris* (*L. longirostris*, order Siluriformes, family Bagridae), commonly known as the Chinese longsnout catfish, is an endemic and economically important fish species native to the Yangtze River in China. In recent decades, wild populations of this species have undergone a severe decline due to habitat degradation and overfishing. Although artificial propagation techniques have been successfully developed since the early 1990s, low larval survival rates remain a major bottleneck in commercial production. Consequently, improving hatching efficiency and optimizing larval rearing techniques are considered critical for the sustainable and efficient aquaculture of *L. longirostris*.

Specifically, research on *L. longirostris* primarily focuses on artificial propagation, diseases, gonadal development, nutrient metabolism, intestinal microbiota, ecological populations, and molecular biology[1-13]. In contrast, studies on its embryonic development are relatively limited[14-16]. Additionally, owing to limitations in imaging technology in the early 1990s, clear and systematic photographs of embryonic and larval development are lacking. Furthermore, advances in molecular techniques have renewed interest to the reproductive biology and larval rearing of *L. longirostris*. Thus, detailed morphological observation and documentation of embryonic and larval development via microscopic photography will not only improve our understanding of early ontogenetic processes but also provide fundamental data for investigating mechanisms such as sexual differentiation during development.

The initial feeding period represents the stage with the highest mortality rates during larval rearing. Blaxter and Hempel[17] first proposed the concept of the "Point of No Return" (PNR), defined as the critical threshold beyond which starved larvae can no longer regain feeding capacity, even if they survive for a limited period thereafter. Extensive research has been conducted on the starvation tolerance and the determination of PNR in larvae to determine the PNR in various fish species, including *Dentex tumifrons*, *Misgurnus anguillicaudatus*, *Hucho taimen*, *Alosa sapidissima*, *Carassius auratus* red var., *Siniperca scherzeri*, *Lateolabrax maculatus*, *Phoxinus lagowskii*, *Hapalogenys mucronatus*, *Odontobutis yaluensis*, *Opsariichthys bidens*, and *Procypris merus*[18-29]. These findings have significantly contributed to the optimization of larval rearing strategies. In this study, we observed and recorded embryonic and larval development, and then investigated the timing of first feeding and the PNR in *L. longirostris*. Thus, this study elucidates the feeding behavior and growth patterns during the early ontogeny of *L. longirostris*, thereby improving our biological and physiological understanding of the species and providing a scientific basis for optimizing larval rearing practices.

# 1 Material and Methods

## 1.1 Materials

Broodstock of *L. longirostris* were obtained from the Center for Conservation and Utilization of Rare and Endemic Fishes in Sichuan. The experimental broodstock included three females (one 7-year-old with a total length of 68.2 cm, and two 9-year-old with total lengths of 76.2 and 78.4 cm) and one male (5-year-old with a total length of 57.4 cm). The experiment was conducted at the aquaculture laboratory of the center.

## 1.2 Experimental Design

### 1.2.1 Fertilized egg collection and incubation

On April 12, 2024, the broodstock were induced to spawn via hormonal injection. Artificial fertilization was performed using the dry method on the following day, whereupon the eggs were uniformly spread onto nylon mesh substrates and subsequently incubated in aerated water. Specifically, the fertilized eggs were reared in a thermostatic glass aquarium maintained at a water temperature of (24.5 ± 0.5) ℃ and a pH of 7.0 ± 0.5. Additionally, a continuous flow-through filtration system was employed with constant aeration to maintain adequate dissolved oxygen levels.

### 1.2.2 Embryonic development observation

Before the formal experiment, two preliminary trials were performed to determine the observation schedule. After fertilization, eggs were sampled at 10-min intervals, and ten fertilized eggs were carefully collected and placed on a glass slide for observation under a microscope (Leica DM750 M). Meanwhile, images were captured using a digital camera attached to the microscope. However, the sampling frequency was adjusted to 30-min intervals after the blastula stage and 120-min intervals following the gastrula stage. Referring to the criteria established for *Hypophthalmichthys molitrix*[30], an embryonic developmental stage was identified when 50% of the observed embryos displayed the typical morpho-

logical characteristics of that stage[30].

1.2.3 Larval development observation and starvation experiment

Newly hatched larvae were divided into three experimental groups (Groups A, B, and C) and reared without feeding until death. For Group A (with three replicates), mortality was recorded daily at 14:00 via visual inspection. Dead larvae were removed immediately, and the time to 100% mortality was documented. For Group B, 60 larvae were randomly sampled daily at 14:30 and evenly assigned to three 500 mL beakers (20 larvae per beaker). Newly hatched *Artemia nauplii* were provided as food, and the number of larvae that had ingested prey was recorded 15 min after feeding. Group C was used for morphological analysis: ten larvae were randomly collected daily at 10:00, anesthetized with MS-222, placed on glass slides, and observed under a microscope.

Images were captured under a Leica DM750 M microscope equipped with a micrometer eyepiece. The total length of the larvae, as well as the major and minor axes of their yolk sacs, were measured. Key morphological characteristics at each observation time point were systematically recorded.

The yolk sac of *L. longirostris* is elliptical in shape, and its volume ($V$) was calculated using the formula:

$$V=(4/3)\pi(r/2)^2R/2, \quad (1)$$

where $r$ denotes the minor axis of the yolk sac and $R$ denotes the major axis.

The initial feeding rate (IFR) was calculated using the following formula:

$$\text{IFR}\ (\%) = (N_f / N_t) \times 100, \quad (2)$$

where $N_f$ represents the number of larvae with food observed in the intestine, and $N_t$ denotes the total number of larvae sampled.

The PNR was defined as the age (days post-hatching, dph) at which the initial feeding rate decreased to 50% of its peak value after reaching the maximum feeding rate[31].

### 1.3 Data Processing and Statistical Analysis

Data are presented as the mean ± standard deviation (mean ± SD). Regression analysis was performed using SPSS 26.0 to evaluate the relationships between larval age and both growth parameters and yolk sac volume. Figures were plotted using Microsoft Excel 2016. Images were processed using Adobe Photoshop.

## 2 Results

### 2.1 Embryonic and Larval Development

The fertilized eggs of *L. longirostris* were spherical, transparent, and pale yellow in color. After water absorption and swelling, the egg diameter reached (3.46 ± 0.16) mm, and the eggs exhibited strong adhesiveness. The embryonic incubation period was 68-70 h at a controlled water temperature of (24.5 ± 0.5) ℃. Morphological characteristics during embryonic and larval development are shown in Fig. 1, and the corresponding developmental sequence is summarized in Table 1.

2.1.1 Fertilized egg stage

After fertilization and water absorption (Fig. 1(a)), the cytoplasm gradually accumulated toward the animal pole and separated from the yolk to form a prominent blastodisc within 1 hour post-fertilization (hpf) (Fig. 1(b)).

2.1.2 Cleavage stage

At 1.55 hpf, the blastodisc had cleaved into two equally sized cells, defining the 2-cell stage (Fig. 1(c)). Subsequent divisions continued, and the 4-cell stage was achieved 0.67 h later (Fig. 1(d)), followed by the 8-cell stage after 0.51 h (Fig. 1(e)). Subsequently, the 16-cell stage was achieved 0.44 h later (Fig. 1(f)), and then the 32-cell stage was achieved 0.23 h later (Fig. 1(g)). Finally, the late cleavage phase was reached 0.75 h later (Fig. 1(h)). Throughout the cleavage process, progressive cleavage of the blastodisc led to a continuous increase in cell number and a decrease in individual cell size.

2.1.3 Blastula stage

At 6.83 hpf, the formation of a cap-like protrusion at the animal pole of the egg was observed, marking the entry into the early blastula stage (Fig. 1(i)). After 0.93 h, the blastoderm flattened, transitioning to the mid-blastula stage (Fig. 1(j)). With continued division, the surface cells of the blastula began to epibolize over the yolk mass 1.37 h later, signifying the onset of the late blastula stage (Fig. 1(k)).

2.1.4 Gastrula stage

At 10.79 hpf, the germ ring became visible at the margin where the blastoderm had epibolized halfway (1/2) over the yolk mass, indicating the onset of the early gastrula stage (Fig. 1(l)). After 2.75 h, as epiboly proceeded to cover two-thirds (2/3) of the yolk, a prominent embryonic shield formed, characterizing the mid-gastrula stage (Fig. 1(m)). Following an additional 2.58 h, epiboly advanced to three-quarters (3/4) completion, marking the transition into the late gastrula stage (Fig. 1(n)).

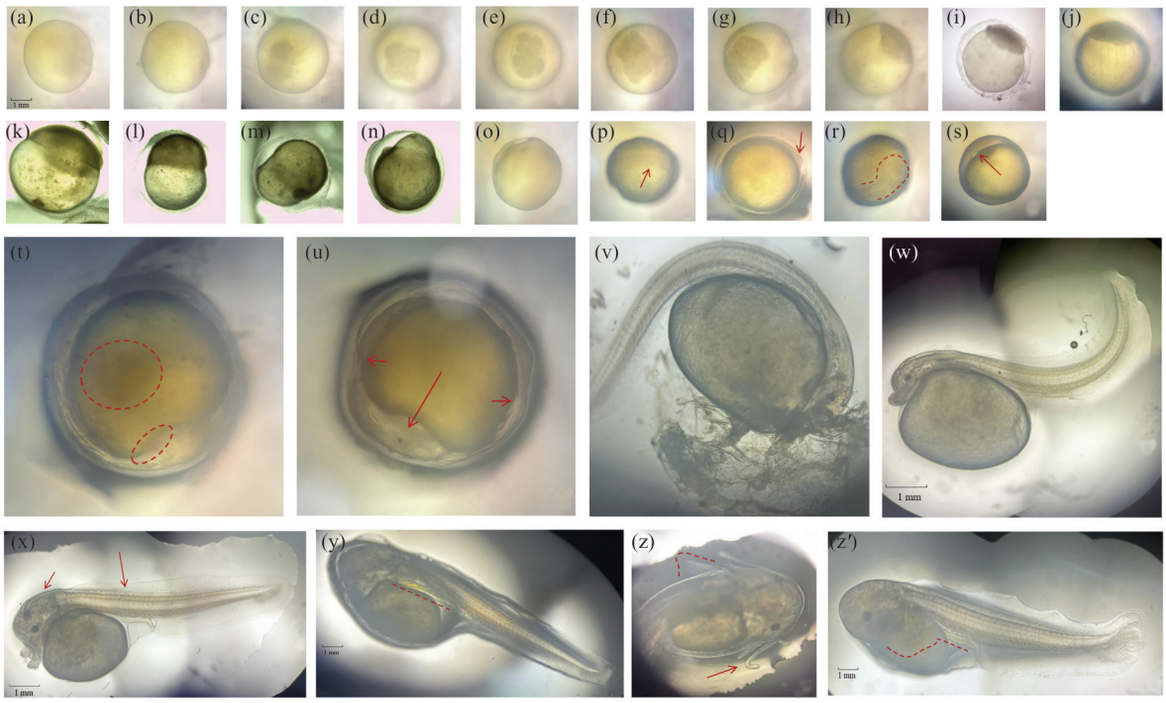


**Fig. 1 Embryonic and larva development of *L. longirostris***

(a) swollen fertilized eggs, (b) blastodisc formation, (c) 2-cell stage, (d) 4-cell stage, (e) 8-cell stage, (f) 16-cell stage, (g) 32-cell stage, (h) mulberry embryos, (i) high blastula stage, (j) middle blastula stage, (k) low blastula stage, (l) early gastrula stage, (m) middle gastrula stage, (n) late gastrula stage, (o) neurula stage, (p) muscle burl stage, (q) optic vesicle stage, (r) tail bud stage, (s) muscular effect stage, (t) heart beating stage, (u) pre-hatching stage, (v) and (w) hatching stage, (x) appearance of body pigments stage, (y) and (z) formation of the intestinal tract stage, (z') first coiling of the intestinal tube stage.

2.1.5 Neurula stage

At 18.00 hpf, the blastoderm completely enveloped the vegetal pole, accompanied by the closure of the blastopore, marking the completion of gastrulation (Fig. 1(o)).

2.1.6 Organ formation stage

At 22.65 hpf, paired somites became evident dorsally along the embryonic axis (Fig. 1(p)). After 2.89 h, the optic primordia emerged bilaterally within the cephalic region (Fig. 1(q)). Following an additional 1.71 h, the tail bud differentiated at the posterior end of the embryo and began to extend away from the yolk sac (Fig. 1(r)). After 6.61 h, intermittent muscular contractions were observed, indicating the onset of the muscular response period (Fig. 1(s)). Subsequently, after 13.66 h, red blood cells became visible in the cardiac region and within the mid-portion of the yolk sac, accompanied by the establishment of a functional circulatory system (Fig. 1(t)).

2.1.7 Pre-hatching stage

At 67.00 hpf, the embryo entered the pre-hatching stage, characterized by observable rotational movements and vigorous tail swings (Fig. 1(u)).

2.1.8 Hatching stage

At 68.00 hpf, intensified tail swings of most embryos led to chorion rupture and subsequent hatching (Fig. 1(v)). Apparently, hatching was completed within 1 h. Newly hatched larvae displayed distinct melanin-deposited eyes and a large ventral yolk sac, exhibiting continuous swimming behavior through active tail motion (Fig. 1(w)).

2.1.9 Larval pigment appearance stage

At 24 h post-hatching (92.00 hpf), melanophores gradually became visible dorsally from the head to the tail region in newly hatched *L. longirostris* larvae. Meanwhile, the heart was positioned beneath the head, closely adjacent to the yolk sac. Both the heart and the cardinal vein within the body cavity were filled with red blood cells. Additionally, a clear blood circulation was observed between the heart and the yolk sac. Details are shown in Fig. 1(x).

2.1.10 Intestinal tract formation stage

At 72 h post-hatching (140.00 hpf), a notable reduction in yolk sac volume was observed. Besides, a straight, light-yellow intestinal tract had developed between the yolk sac and the body (Fig. 1(y)). Concurrently, distinct transparent fan-shaped pectoral fins were clearly visible, as well as maxillary barbels (Fig. 1(z)).

**Table 1 Time table of *L. longirostris* embryonic and larvae development**

| Stage of development | | Time after fertilization/hpf | Figure |
|---|---|---|---|
| The fertilized eggs have hydrated | fertilized eggs become swollen | 0 | 1(a) |
| The fertilized egg stage | cytoplasm becomes concentrated at the animal pole | 1.00 | 1(b) |
| The cleavage stage | 2-cell stage | 1.55 | 1(c) |
| | 4-cell stage | 2.22 | 1(d) |
| | 8-cell stage | 2.73 | 1(e) |
| | 16-cell stage | 3.17 | 1(f) |
| | 32-cell stage | 3.40 | 1(g) |
| | mulberry embryos | 4.15 | 1(h) |
| The blastocyst stage | high blastula stage | 6.83 | 1(i) |
| | middle blastula stage | 7.76 | 1(j) |
| | low blastula stage | 9.13 | 1(k) |
| The gastrula stage | early gastrula stage | 10.79 | 1(l) |
| | middle gastrula stage | 13.54 | 1(m) |
| | late gastrula stage | 16.12 | 1(n) |
| The neurula stage | closure of blastopore | 18.00 | 1(o) |
| The organ formation stage | muscle burl stage | 22.65 | 1(p) |
| | optic vesicle stage | 25.54 | 1(q) |
| | tail bud stage | 27.25 | 1(r) |
| | muscular effect stage | 33.86 | 1(s) |
| | heart beating stage | 47.52 | 1(t) |
| The pre-hatching stage | embryo rotating stage | 67.00 | 1(u) |
| The hatching stage | newly hatched larvae | 68.00 | 1(v), 1(w) |
| The appearance of body pigments stage | onset of pigmentation | 92.00 | 1(x) |
| Formation of the intestinal tract stage | straight digestive tract | 140.00 | 1(y), 1(z) |
| First coiling of the intestinal tube stage | formation of the first intestinal coiling | 164.00 | 1(z') |

2.1.11 First intestinal coiling stage

At 96 h post-hatching (164.00 hpf), the intestinal tract was observed to sink into the yolk sac and form the first coiling, while the caudal region differentiated into discernible fin rays (Fig. 1(z′)).

## 2.2 Yolk Absorption and Larval Growth

The yolk sac of newly hatched *L. longirostris* larvae was elliptical, with a major axis ($R$) of (3.24 ± 0.22) mm, a minor axis ($r$) of (2.80 ± 0.09) mm, and a volume of (13.26 ± 0.86) mm³. The total length of the larvae was (7.52 ± 0.29) mm. Additionally, the yolk sac gradually decreased in size daily, while the total length of the larvae increased steadily. By 9 dph (April 24), the yolk was completely absorbed, and the total length reached (16.26 ± 0.12) mm. Changes in the major and minor axis of the yolk sac are illustrated in Fig. 2.

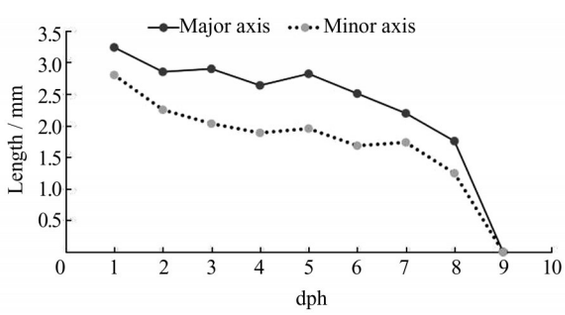


**Fig. 2 Changes in yolk sac major axis and minor axis of *L. longirostris* with dph**

The yolk sac volume ($V$) exhibited a functional relationship with days post-hatching ($d$) (Fig. 3), and the regression equation was as follows and the coefficient of determination $R^2$=0.895 4:

$$V = -0.085\ 6d^3 + 1.385\ 3d^2 - 7.692\ 8d + 19.085. \quad (3)$$

The total length ($L$) of *L. longirostris* demonstrated a functional relationship with days post-hatching ($d$, $1 \leqslant d \leqslant 9$) (Fig. 4), described by the following regression

equation and $R^2 = 0.8940$:

$$L = 0.053\ 7d^2 + 0.500\ 9d + 7.231\ 6. \quad (4)$$

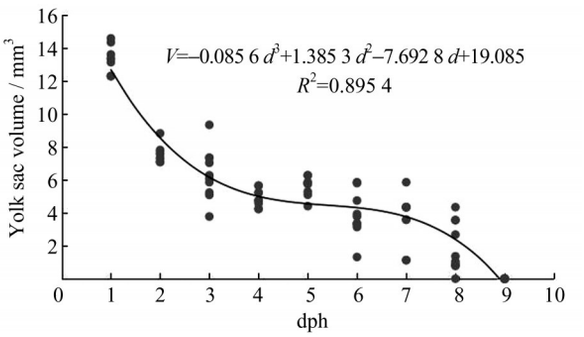


**Fig. 3 Changes in yolk sac volume of *L. longirostris* with dph**

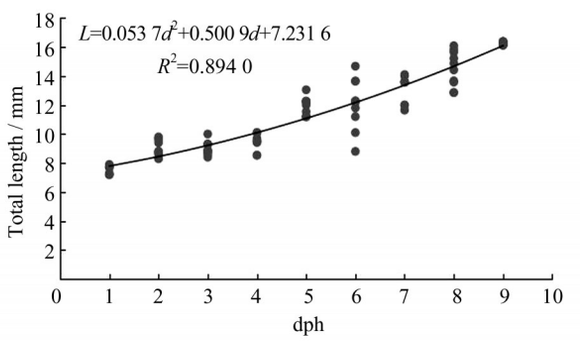


**Fig. 4 Changes in total length of *L. longirostris* with dph**

### 2.3 Initial Feeding Rate and PNR

Results from the starvation trials (Groups A and B) indicated that all *L. longirostris* larvae died by 16-17 dph at a water temperature of (24.5 ± 0.5) °C. As shown in Fig. 5, the initial feeding rate was (63.33 ± 2.89)% in 5-dph larvae, reached 100% in 8-dph larvae, and remained at this level for four consecutive days. From 11 to 16 dph, the initial feeding rate gradually decreased with starvation, dropping to (33.33 ± 5.77)% in 16-dph larvae, which was the first time it fell below 50% of the maximum initial feeding rate.

## 3 Discussion

### 3.1 Embryonic and Larval Development

Based on the criteria established for embryonic and larval developmental staging in *Hypophthalmichthys molitrix*[29], *Pangasianodon hypophthalmus*[31], and *Carassius auratus*[32], the present study delineated the embryonic and larval development of *L. longirostris* based on its specific developmental characteristics.

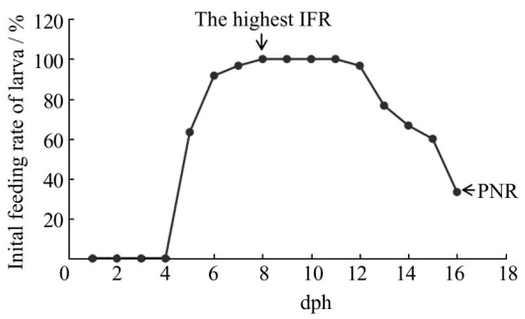


**Fig. 5 Changes in initial feeding rate of *L. longirostris* with dph**

Clear and well-defined developmental photographs were got, capturing distinct morphological features throughout ontogeny. Specifically, embryonic development was divided into eight consecutive phases: fertilized egg, cleavage, blastula, gastrula, neurula, organ formation, pre-hatching, and hatching. Subsequently, post-hatching larval development was characterized by three key stages: the appearance of body pigments, formation of the intestinal tract, and first coiling of the intestinal tube. Accurately, embryonic development in *L. longirostris* proceeded through typical discoidal meroblastic cleavage, leading to the formation of a discoidal blastula. Subsequent gastrulation occurred via epiboly, followed by further differentiation into larval structures. And during the initial four days post-hatching, larvae exhibited preliminary development of key organs, including the digestive tract, mouth, eyes, barbels, and fin folds. Notably, newly hatched *L. longirostris* larvae remain in a critical period of ongoing organogenesis. Therefore, in aquaculture practice, optimal water conditions should be ensured during this stage to promote larval development and enhance survival rates.

The fertilized eggs of *L. longirostris* reached a diameter of (3.46 ± 0.16) mm after water absorption, which is comparable to that of *Ictalurus punctatus* (3.5-4.0 mm)[34] but significantly larger than those of *Pangasianodon hypophthalmus* ((1.60 ± 0.23) mm) [32], and *Carassius auratus* (1.53-1.73 mm)[33], demonstrating notable interspecific variation in egg size among teleosts. Additionally, regarding developmental timing, preliminary trials showed a hatching period of 70-73 h for an earlier batch of *L. longirostris* under consistent conditions, while Zhang *et al*[15] reported durations of 64.83 h at 25 ℃ and 75.02 h at 23 ℃, and the current study observed a range of 68-70 h, which suggest that parental origin may cause minor intraspecific variations in incu-

bation duration. Furthermore, even among closely related bagrid catfishes, embryonic development rates varied considerably, for example, *Pelteobagrus fulvidraco* required 102.6 h to hatch at 25 ℃[35], markedly longer than *L. longirostris*.

### 3.2 Yolk Absorption and Larval Growth

The starvation experiment revealed that *L. longirostris* larvae relied exclusively on endogenous yolk nutrition until 5 dph, entered a mixed nutrition phase from 5 to 9 dph, and transitioned to full exogenous feeding after yolk depletion at 9 dph. High $R^2$ values (>0.89) of Equations (3) and (4) indicated robust regression model fitting. Equation (3) demonstrated a slower yolk absorption rate during the mixed phase, suggesting reduced yolk dependency after initial feeding. In addition, equation (4) reflected accelerated post-feeding growth, marking a shift to rapid development. Moreover, compared to species with smaller eggs such as *Carassius auratus*[36], *Culter alburnus*[37], and *Chanodichthys erythropterus*[38] (egg diameter: 0.94-1.50 mm), *L. longirostris* (egg diameter: 3.46 mm) had a pure endogenous nutrition period that is one-day longer, likely due to its larger yolk reserves. These results emphasize the need for timely provision of suitable live feed at the conclusion of endogenous nutrition in larval culture practice.

### 3.3 Initial Feeding Rate and PNR

The initial feeding rate and sustained maximum feeding rate period reflect larval feeding ability, and the PNR serves as a critical threshold for starvation tolerance, beyond which feeding capacity becomes irreversibly impaired even if survival briefly continues[17]. As shown in Table 2, the initial feeding rate was higher in *L. longirostris* than in other reported species such as *Dentex tumifrons*, *Misgurnus anguillicaudatus*, *Hucho taimen*, *Alosa sapidissima*, *Carassius auratus* Red variety, *Siniperca scherzeri*, *Lateolabrax maculatus*, *Phoxinus lagowskii*, *Hapalogenys mucronatus*, *Odontobutis yaluensis*, *Opsariichthys bidens*, and *Procypris merus*[18-29], indicating a strong early demand for exogenous nutrition. Subsequently, larvae reached 100% feeding rate from 8 to 11 dph, demonstrating strong feeding capacity. Although yolk depletion occurred by 9 dph, the PNR was reached as late as 16 dph, suggesting strong starvation tolerance of *L. longirostris.* Overall, it may attributable to ample yolk reserves of *L. longirostris* that support enhanced larval development and feeding capacity. Finally, mortality increased rapidly after PNR, with larvae surviving less than one day beyond this point, highlighting its importance in defining feeding schedules during *L. longirostris* larval culture.

**Table 2 Table of some larvae's initial feeding rate and PNR**

| Species | *T*/℃ | Days old at initial feeding/dph | Feeding rate on initial feeding day/% | Period of maximal initial feeding rate/dph | Maximal initial feeding rate/% | PNR/dph | Reference |
|---|---|---|---|---|---|---|---|
| *Leiocassis longirostris* | 24.0-25.0 | 5 | 63.33 | 8-11 | 100 | 16 | This study |
| *Procypris merus* | 20.0-22.0 | 5 | 15.00 | 8-14 | 100 | 19 | [29] |
| *Opsariichthys bidens* | 20.5-22.5 | 10 | 55.56 | 11 | 88.00 | 12-13 | [28] |
| *Odontobutis yaluensis* | 19.7-23.2 | 1 | 40.00 | 2-8 | 100 | 12-13 | [27] |
| *Hapalogenys mucronatus* | 23.8-24.2 | 3 | 10.12 | 7 | 85.06 | 7-8 | [26] |
| *Phoxinus lagowskii* | 16.0-18.0 | 7 | 36.36 | 9 | 85.71 | 14 | [25] |
| *Lateolabrax maculatus* | 20.0-22.0 | 4 | 10.00 | 8 | 86.67 | 9-10 | [24] |
| *Siniperca scherzeri* | 22.0-24.0 | 3 | 5.00 | 6 | 85.00 | 7-8 | [23] |
| *Carassius auratus* Red variety | / | 4 | 6.67 | 7 | 100 | 8-9 | [22] |
| *Alosa sapidissima* | 19.5-21.5 | 3 | 46.67 | 5 | 89.29 | 7-8 | [21] |
| *Hucho taimen* | 10.0-12.0 | 21 | 10.00 | 29-34 | 100 | 39-40 | [20] |
| *Misgurnus anguillicaudatus* | 21.4-24.8 | 3 | 28.57 | 5 | 88.00 | 10 | [19] |
| *Dentex tumifrons* | 21.0-23.0 | 4 | 10.00 | 7 | 75.00 | 8-9 | [18] |

Note：/ means no data.

# 4 Conclusion

In conclusion, at a water temperature of (24.5 ± 0.5) ℃, the fertilized eggs of *L. longirostris* hatched into larvae within 68-70 h. Embryonic development could be divided into eight distinct stages: fertilized egg, cleavage, blastula, gastrula, neurula, organ formation, pre-hatching, and hatching. Before initial feeding, three key developmental phases were observed in newly hatched larvae: the appearance of body pigments, the formation of the intestinal tract, and the first coiling of the intestinal tube. Furthermore, initial feeding of the larval occurred at 5 dph, with a feeding rate of (63.33 ± 2.89)%. The feeding rate reached 100% between 8 and 11 dph, and the PNR was 16 dph. In summary, for the artificial breeding of *L. longirostris*, it is recommended to collect the larvae promptly at 70 hpf and transfer them to rearing tanks. During larval rearing, suitable initial feeding diets should be provided starting at 5 dph.

**Acknowledgements:**

We wish to thank Chen Keyin, Chen Ye, Li Jianqiang, Lou Qiling and Ma Hong for their help in *L. longirostris* artificial breeding.

# References

[1] Yang R B, Li H, Peng S J. Histological observation on ovarian development of *Leiocassis longirostris*[J]. *Sichuan Journal of Zoology*, 1990, **9**(2): 19-20(Ch).

[2] Wang X Q, Mo Y X, Zhong L, *et al*. Histological study on the annual reproductive cycle of *Leiocassis longirostris*[J]. *Freshwater Fisheries*, 2005, **35**(4): 18-20(Ch).

[3] Han X. Artificial propagation technology of *Leiocassis longirostris*[J]. *China Fisheries*, 2024, **5**: 53-55(Ch).

[4] Fan J H, Ye H, Song X H, *et al*. Comparative transcriptomic analysis of male and female gonads of the Chinese longsnout catfish (*Leiocassis longirostris*) [J]. *Journal of Fishery Sciences of China*, 2024, **31**(2): 129-143(Ch).

[5] Zhao Z M, Zhou J, Li Q, *et al*. Analysis and evaluation of nutritive composition in muscles of cultured *Leiocassis longirostris* at different ages[J]. *Chinese Agricultural Science Bulletin*, 2023, **39**(23): 102-108(Ch).

[6] Li Y, Yang Z R, Cheng J H, *et al*. Effects of hypoxia stress and reoxygenation on appetite, hypoxic response genes and physiological and biochemical indexes in the brain tissues of *Leiocassis longirostris*[J]. *Journal of Fisheries of China*, 2023, **47**(1): 152-164(Ch).

[7] Zhang X F. *Effects of Stocking Density on Growth, Biochemical and Immune Indices of Leiocassis longirostris Juveniles in Pond Juanyang Mode*[D]. Wuhan: Huazhong Agricultural University, 2022(Ch).

[8] Xiao Y, Lei Y, Tang S L, *et al*. Identification and antibiotic sensitivity of *Edwardsiella ictaluri* isolated from cultured *Leiocassis longirostris*[J]. *Chinese Journal of Fisheries*, 2015, **28**(1): 39-44(Ch).

[9] Zhu X M, Xie S Q, Lei W, *et al*. Compensatory growth in the Chinese longsnout catfish, *Leiocassis longirostris* following feed deprivation: Temporal patterns in growth, nutrient deposition, feed intake and body composition[J]. *Aquaculture*, 2005, **248**: 307-314.

[10] Liang H W, Guo S S, Luo X Z, *et al*. Molecular diagnostic markers of *Tachysurus fulvidraco* and *Leiocassis longirostris* and their hybrids[J]. *SpringerPlus*, 2016, **5**(1): 2115.

[11] He W P, Zhou J, Li Z, *et al*. Chromosome-level genome assembly of the Chinese longsnout catfish *Leiocassis longirostris*[J]. *Zool Res*, 2021, **42**(4): 417-422.

[12] Liu M, Zhou Y L, Guo X F, *et al*. Comparative transcriptomes and metabolomes reveal different tolerance mechanisms to cold stress in two different catfish species[J]. *Aquaculture*, 2022, **560**: 738543.

[13] Zhao Z M, Zhao H, Wang X Y, *et al*. Effects of different temperatures on *Leiocassis longirostris* gill structure and intestinal microbial composition[J]. *Scientific Reports*, 2024, **14**(1): 7150.

[14] Su L D, He X F, Pu D Y, *et al*. A preliminary observation on the embryonic development of *Leiocassis longirostris*[J]. *Freshwater Fisheries*, 1985, **4**: 2-4(Ch).

[15] Zhang Y G, He X F, Pu D Y. The relationship between temperature and embryonic and larval development of *Leiocassis longirostris*[J]. *Journal of Fisheries of China*, 1991, **15** (2): 172-176(Ch).

[16] Liu X L, Jin L, Zhang Y G. Effects of salinity and pH on embryonic development of *Leiocassis longirostris*[J]. *Journal of Anhui Agricultural Sciences*, 2013, **41**(8): 3422-3423(Ch).

[17] Blaxter J H S, Hempel G. The influence of egg size on herring larvae (*Clupea harengus* L.) [J]. *Journal du Conseil*, 1963, **28**(2): 211-240.

[18] Xia L J, Shi Z H, Lu J X. Experimental starvation on *Dentex tumifrons* larvae and definition of the point of no return[J]. *Marine Fisheries*, 2004, **26**(4): 286-290(Ch).

[19] Wang Y J, Song L M, Yao R R, *et al*. Determination of the point of no return (PNR) in loach (*Misgurnus anguillicaudatus*) larvae[J]. *Journal of Hydroecology*, 2007, **6**: 17-20(Ch).

[20] Zhang Y Q, Yin J S, D J, *et al*. Experimental starvation on *Hucho taimen* and definition of the point of no return[J]. *Acta Hydrobiologica Sinica*, 2009, **33**(5): 945-950(Ch).

[21] Gao X Q, Hong L, Liu Z F, *et al*. The definition of point of no return of larvae and feeding characteristics of *Alosa sapi-*

*dissima* larvae and juveniles[J]. *Journal of Fisheries of China*, 2015, **39**(3): 392-400(Ch).

[22] Xu Z C, Wang G C, Liu Q, *et al*. Experimental starvation on Gold Crucian Carp larvae and determination of the point of no return[J]. *Journal of Aquaculture*, 2015, **36**(4): 14-19(Ch).

[23] Wang M Y. Starvation test on *Siniperca scherzeri* Larvae and acertaining the point of no return[J]. *Journal of Guangdong Ocean University*, 2015, **35**(4): 99-103(Ch).

[24] Wang X L, Wen H S, Zhang M Z, *et al*. Determination of irreversible starvation point and feeding rhythm of *Lateolabrax maculatus* larvae[J]. *Periodical of Ocean University of China*, 2017, **47**(5): 57-64(Ch).

[25] Ren X Y, Luo X N, Deng S P, *et al*. Development of larva, irreversible starvation point and optimal stocking time of *Phoxinus lagowskii* larva[J]. *Fisheries Science*, 2023, **42**(4): 594-603(Ch).

[26] Fu T Z, Ping H L, Zhang T, *et al*. Study on the irreversible starvation point and feeding growth characteristics of *Hapalogenys mucronatus* larvae[J]. *Oceanologia et Limnologia Sinica*, 2022, **53**(6): 1494-1502(Ch).

[27] Li W K, Luo X N, Duan Y J, *et al*. Observation on development of larvae and determination of point of no return in sleeper (*Odontobutis yaluensis*)[J]. *Journal of Dalian Ocean University*, 2023, **38**(1): 32-42(Ch).

[28] Xing Y X, Luo X N, Li J, *et al*. Observation of early development and determination of the point of no return (PNR) in Chinese hook snout carp (*Opsariichthys bidens*)[J]. *Journal of Dalian Ocean University*, 2023, **38**(6): 972-979(Ch).

[29] Li J, Yang B, Dong W W, *et al*. Feeding and starvation tolerance of yolk-sac larvae of *Percocypris mera*[J]. *Journal of Hydroecology*, 2023, **44**(2): 89-95(Ch).

[30] Lou Y D. *Histology and Embryology*[M]. Beijing: China Agriculture Press, 2002: 347-354(Ch).

[31] Yin M C. Research and progress in fish early life history[J]. *Journal of Fisheries of China*, 1991, **15**(4): 348-358(Ch).

[32] Ni W, Chen H G, Liu X L, *et al*. Embryonic development and growth of larval and juvenile basa fish striped catfish (Pangasianodon hypophthalmus) and the determination of growth model[J]. *Journal of Dalian Ocean University*, 2023, **38**(4): 584-592(Ch).

[33] Wang J N, Tai D M, Zhou C Q, *et al*. Preliminary study on embryo and juvenile development of *Carassius auratus*[J]. *Northern Chinese Fisheries*, 2023, **42**(1): 9-13(Ch).

[34] Cao J Y, Liu J K, Liu X T, *et al*. Study on embryonic development of channel catfish (*Ictalurus punctatus*)[J], *Freshwater Fisheries*, 1993, **23**(1): 41-42(Ch).

[35] Yuan L Q, Xie X J, Cao Z D, *et al*. Effects of temperature on embryonic development of darkbarbel catfish *Pelteobagrus vachelli*[J]. *Acta Zoologica Sinica*, 2005, **51**(4): 753-757(Ch).

[36] Liang Z Q, Ma S, Yao J J, *et al*. The embryonic development of Puan Crucian Carp *Carassius auratus* Linnaeus[J]. *Fisheries Science*, 2012, **31**(6): 316-320(Ch).

[37] Huang Y L, Peng M, He A Y, *et al*. Embryonic development of *Culter alburnus*[J]. *Journal of Guangxi Academy of Sciences*, 2005, **21**(3): 148-150(Ch).

[38] Yin H C, Lv H Y. Artificial propagation and embryonic development in *Ancherythroculter nigrocauda*[J]. *Journal of Dalian Ocean University*, 2010, **25**(3): 265-269(Ch).

# 长吻鮠胚胎、仔鱼发育观察及饥饿不可逆点的确定

钱静[1]， 魏震[2]， 郑维[2†]， 熊银林[2]， 蒋梦皞[2]， 李娜[1]， 陶敏[1]， 覃川杰[1]

1. 内江师范学院 长江上游鱼类资源保护与利用四川省重点实验室,四川 内江 641100

2. 四川省珍稀特有鱼类保护与利用中心,四川 成都 611247

**摘要：**为研究长吻鮠(*Leiocassis longirostris*)胚胎发育和仔鱼发育特点，确定仔鱼饥饿不可逆点(Point of No Return, PNR)，在水温(24.5 ± 0.5) ℃条件下孵化受精卵，用显微镜观察其胚胎和仔鱼发育时序特征，并开展初孵仔鱼的饥饿试验，研究长吻鮠仔鱼的形态发育、生长特征及摄食能力。结果表明，长吻鮠受精卵吸水膨胀后卵径为(3.46 ± 0.16) mm，68-70 h孵化出膜。胚胎历经受精卵期、卵裂期、囊胚期、原肠期、神经胚期、器官形成期、出膜前期和出膜期8个阶段。初孵仔鱼开口前，可观察出体色素出现、肠管建成和肠管弯曲期3个阶段。4日龄内长吻鮠仔鱼为内源性营养阶段，5日龄长吻鮠仔鱼初次开口，摄食率为(63.33 ± 2.89)%，开始混合性营养阶段，9日龄卵黄吸收完全，转为依赖外源性营养。8~11日龄摄食率为100%，之后开始减小，PNR为16日龄。16-17日龄仔鱼因饥饿全部死亡。因此，长吻鮠仔鱼最佳初次投喂时间在5日龄。本研究结果为长吻鮠早期发育阶段的探索提供了基础资料，对于高效苗种培育具有实践意义。

**关键词：**长吻鮠；胚胎发育；仔鱼发育；饥饿不可逆点

□